МІНЕРАЛОГІЧНИЙ ЖУРНАЛ
MINERALOGICAL JOURNAL
(UKRAINE)

UDK 549.643.25:539.122

**V. P. Ivanitskiy, K. O. Ilchenko, G. V. Legkova,
P. O. Voznyuk, A. S. Lytovchenko, A. L. Litvin**

Octahedral cations distribution in the structure of magnesiohastingsite. Kinetics of structural iron radiation oxidation

The distribution of octahedral cations within nonequivalent sites of magnesiohastingsite structure has been investigated by means of *X*-ray structural analysis, NGR- and IR-spectroscopy. Variations of ferrous and ferric ions contents in different structural sites and kinetics of Fe^{3+} ions accumulation in the course of γ-irradiation are described by mathematical equations. The calculated kinetic parameters enabled to estimate the minerals susceptibility to radiation action. Dependence of the radiation effects on the irradiated mineral particles size has been found. The radiation oxidation of iron takes place mainly in *M*1 and *M*3 sites, adjacent to *A* sites occupied by K^+ and Na^+ ions. Probable mechanisms of radiation oxidation, thermal reduction of iron ions and dehydroxylation of their structural environment are proposed. The results obtained may be used for dosimetry of radiation loads and for estimation of the amphibole-bearing rocks fitness capabilities for burying the radioactive waste products.

Introduction. Intense development of atomic engineering and radionuclides application in industry, medicine and other fields of human activity puts forward problems of development of technologies of radioactive wastes (RW) safe storage and diminution of their influence on the environment. The modern technologies of RW burial use natural and synthetic mineral substances. It stimulates development of investigations of the radiation influence on the structural state of minerals and rocks as materials of engineering designs and constructions for RW storage. Minerals and rocks suitability for these purposes is based on their radiation structural stability.

Amphiboles belong to the most widespread minerals of the earthÿs crust. They constitute about 7 volume percent of magmatic, metamorphic and metasomatic rocks [14]. Since amphiboles have some elements of variable valence in their structure, they are sensitive to the radiation influence. The radiation influence on structure and some physicochemical properties of amphiboles were investigated in a series of scientific publications [6–8, 11, 12, 18, 19].

Purposes, objects and analytical methods. To clear up the dependence of amphiboles radiation stability from their composition and to continue our previous works on this topic [6–8, 18, 19], octahedral cations distribution in the structure of magnesiohastingsite and irradiation influence on iron cations valence state and on their anionic environment study is carried out.

Chemical composition of studied amphibole in % is: SiO_2 — 41.71; TiO_2 — 1.28; Al_2O_3 — 10.33; Fe_2O_3 — 5.87; FeO — 15.20; MnO — 0.45; MgO — 8.79; CaO — 12.25; Na_2O — 1.25; K_2O — 1.00; H_2O^- — 0.20; H_2O^+ — 1.93; F — 0.11; *the sum* — 100.33 (sample from granodiorite Trigur massif, Volyn', Ukraine, v. Grigor'je, collection of A. L. Litvin). The crystallochemical formula of amphibole, calculated by the "Minfile" program per 13 of cations, is:

$$(Na_{0.37}K_{0.19})_{0.56}(Ca_{2.00})_{2.00}(Mg_{1.99}Mn_{0.06}Fe^{2+}_{1.94}Fe^{3+}_{0.66}Al_{0.20}Ti_{0.15})_{5.00}(Si_{6.35}Al_{1.65})_{8.00}O_{22.00}(OH)_{2.00}.$$

According to mineralogical classification [21] amphibole under consideration is magnesiohastingsite.

The crystal lattice parameters and structure-forming elements distribution are obtained by means of *X*-ray structural analysis. To control the iron cations distribution between octahedral structural sites and their valence state nuclear gamma-resonance (NGR) is used. The state

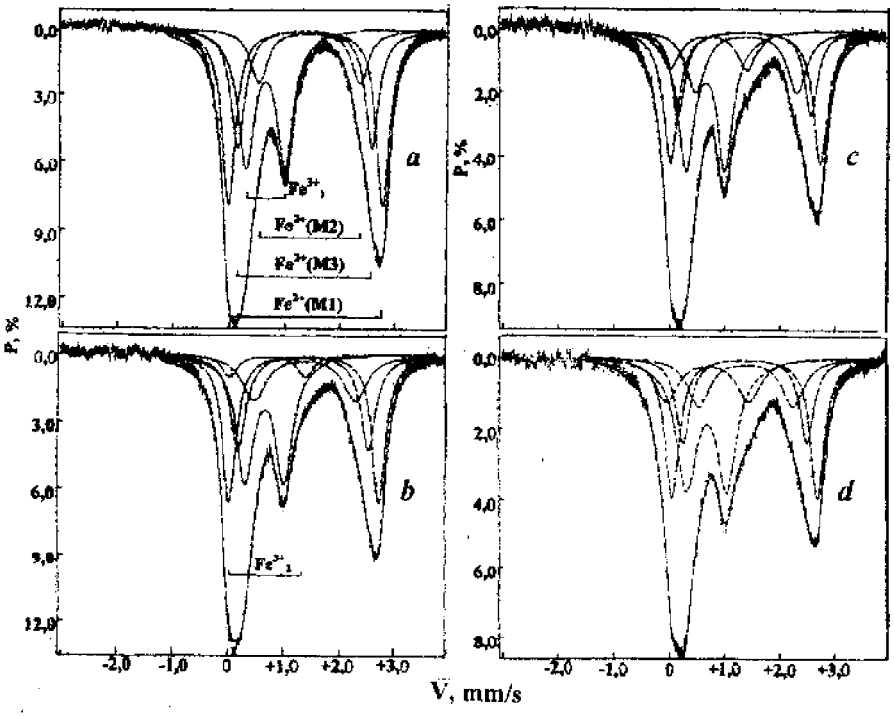

Fig. 1. Spectra NGR magnesiohastingsite: *a* – *d* — samples initial and irradiated by dozes $1 \cdot 10^8$, $2 \cdot 10^8$, $4 \cdot 10^8$ Gy accordingly. The strokes show a situation of lines of absorption of the allocated doublets

of OH-groups depending on its nearest cationic environment is studied by infra-red (IR) spectroscopy.

Samples were irradiated by ^{60}Co source, and also by placing amphibole samples in the wet channel of nuclear reactor fuel assembly storehouse. Maximal doze of irradiation (*D*) was $4 \cdot 10^8$ Gy at doze capacity (*P*) 18.05 Gy/s.

Experimental results and discussion. *Refinement of cations distribution.* Structure parameters and sites population in amphiboles of hastingsite series are known to depend on their composition and conditions of formation [16, 17].

Calculated magnesiohastingsite lattice cell parameters (diffractometer DRON-2. radiation $Cu_{K\alpha}$, measurement of E. E. Grechanovskaja, IGMOF NACU) are: $a = 0.9896$ (2) nm, $b = 1.8156$ (20) nm, $c = 0.5321$ (12) nm, $\beta = 105° 25'$ (9'), $v = 0.9233$ nm^3.

Experimental data for structure refinement is obtained on the four-circled automatic diffractometer "ДАРЧ-1". Refinement of "Fe" and "Mg" distribution between octahedral sites *M*1, *M*2 and *M*3 ("Fe" = Fe^{2+}, Fe^{3+}, Mn^{2+}, Ti^{4+} and "Mg" = Mg^{2+}, Al^{3+}) is made by the least squares method. The last was successfully applied to study octahedral cations distribution in amphiboles [16–18]. Refinement of atomic structural positions is carried out by comparison of experimental and calculated interatomic distances in *M*1, *M*2 and *M*3 octahedra, that are equal to (in nm): *M*1–O — 0.2107 and 0.2110; *M*2–O — 0.2049 and 0.2041; *M*3–O — 0.2112 and 0.2113 correspondingly.

The following cations distribution between octahedral structural sites (calculated per one position), based on the sample chemical composition and experimental interatomic distances is received: $M1 = 0.505\ Fe^{2+} + 0.495$ Mg; $M2 = 0.155\ Fe^{2+} + 0.33\ Fe^{3+} + 0.07$ Ti + 0.10 Al + 0.345 Mg; $M3 = 0.68\ Fe^{2+} + 0.32$ Mg.

Mn cations contribution (0.06 u.) is included in the contribution of iron cations. Structural position of Mn cations in amphiboles is ambiguous. The largest value of the average Mn–O distance in octahedral sites *M*1 and *M*2 would be 0.2173 nm [16]. In *M*3 they are 0.001 nm smaller. However the range of average bonds length changes in *M*1 and *M*3 octahedra is approximately half, than that in *M*2. In other words, *M*2 octahedron is more mobile than *M*1 and *M*3. This causes its filling both by small and large cations. At the same time Mn^{2+} ionic radius

Table 1. **Parameters of NGR spectra of magnesiohastingsite**

$D\cdot10^8$ Gy	Ion, site	δ	Δ	*W*	*S*, %	*N*, u.
		mm/s				
0	Fe^{2+}(2*M*1)	1.38	2.78	0.33	31.5	0.82
	Fe^{2+}(*M*3)	1.37	2.40	0.38	24.2	0.63
	Fe^{2+}(2*M*2)	1.41	1.78	0.51	14.2	0.37
	Fe_1^{3+}	0.66	0.71	0.43	30.1	0.78
	Fe_2^{3+}	—	—	—	—	—
0.01	Fe^{2+}(2*M*1)	1.39	2.75	0.33	32.0	0.83
	Fe^{2+}(*M*3)	1.37	2.38	0.40	25.3	0.66
	Fe^{2+}(2*M*2)	1.43	1.74	0.59	15.3	0.40
	Fe_1^{3+}	0.67	0.72	0.38	27.4	0.71
	Fe_2^{3+}	—	—	—	—	—
0.1	Fe^{2+}(2*M*1)	1.39	2.73	0.27	30.5	0.79
	Fe^{2+}(*M*3)	1.37	2.38	0.31	24.2	0.63
	Fe^{2+}(2*M*2)	1.37	1.88	0.37	14.2	0.37
	Fe_1^{3+}	0.66	0.72	0.42	31.1	0.81
	Fe_2^{3+}	—	—	—	—	—
1.0	Fe^{2+}(2*M*1)	1.39	2.72	0.30	28.1	0.73
	Fe^{2+}(*M*3)	1.37	2.37	0.31	21.0	0.55
	Fe^{2+}(2*M*2)	1.40	1.81	0.45	14.4	0.37
	Fe_1^{3+}	0.67	0.73	0.38	30.8	0.80
	Fe_2^{3+}	0.70	1.45	0.39	5.7	0.15
1.3	Fe^{2+}(2*M*1)	1.39	2.71	0.28	27.5	0.72
	Fe^{2+}(*M*3)	1.37	2.33	0.30	20.0	0.52
	Fe^{2+}(2*M*2)	1.41	1.74	0.43	14.7	0.38
	Fe_1^{3+}	0.68	0.72	0.37	30.0	0.78
	Fe_2^{3+}	0.68	1.50	0.40	7.8	0.20
1.6	Fe^{2+}(2*M*1)	1.38	2.71	0.28	26.7	0.70
	Fe^{2+}(*M*3)	1.36	2.34	0.29	19.6	0.51
	Fe^{2+}(2*M*2)	1.39	1.77	0.42	14.4	0.37
	Fe_1^{3+}	0.67	0.70	0.37	29.6	0.77
	Fe_2^{3+}	0.72	1.41	0.52	9.7	0.25
2	Fe^{2+}(2*M*1)	1.39	2.72	0.27	25.6	0.67
	Fe^{2+}(*M*3)	1.37	2.32	0.27	19.0	0.49
	Fe^{2+}(2*M*2)	1.39	1.79	0.43	14.4	0.37
	Fe_1^{3+}	0.67	0.70	0.41	29.0	0.75
	Fe_2^{3+}	0.69	1.37	0.62	12.1	0.32
3	Fe^{2+}(2*M*1)	1.38	2.67	0.31	24.2	0.63
	Fe^{2+}(*M*3)	1.36	2.29	0.35	18.2	0.47
	Fe^{2+}(2*M*2)	1.40	1.76	0.49	14.2	0.37
	Fe_1^{3+}	0.67	0.71	0.41	31.1	0.81
	Fe_2^{3+}	0.70	1.39	0.56	12.3	0.32
4	Fe^{2+}(2*M*1)	1.38	2.66	0.33	24.0	0.62
	Fe^{2+}(*M*3)	1.35	2.32	0.34	17.8	0.46
	Fe^{2+}(2*M*2)	1.38	1.75	0.52	14.1	0.37
	Fe_1^{3+}	0.68	0.73	0.41	34.8	0.90
	Fe_2^{3+}	0.70	1.59	0.43	9.3	0.24
4*	Fe^{2+}(2*M*1)	1.38	2.67	0.27	23.8	0.61
	Fe^{2+}(*M*3)	1.36	2.27	0.28	17.5	0.46
	Fe^{2+}(2*M*2)	1.37	1.72	0.46	13.7	0.36

The End of Table 1.

$D \cdot 10^8$ Gy	Ion, site	δ	Δ	W	S, %	N, u.
		mm/s				
4**	$Fe^{2+}(2M1)$	1.40	2.75	0.30	23.4	0.61
	$Fe^{2+}(M3)$	1.38	2.36	0.31	18.8	0.49
	$Fe^{2+}(2M2)$	1.41	1.78	0.45	13.0	0.34
	Fe_1^{3+}	0.67	0.72	0.41	31.3	0.81
	Fe_2^{3+}	0.71	1.48	0.52	13.5	0.35
4***	$Fe^{2+}(2M1)$	1.39	2.69	0.30	23.0	0.60
	$Fe^{2+}(M3)$	1.37	2.31	0.33	19.2	0.50
	$Fe^{2+}(2M2)$	1.40	1.72	0.49	14.1	0.37
	Fe_1^{3+}	0.68	0.71	0.39	29.0	0.75
	Fe_2^{3+}	0.68	1.49	0.50	14.7	0.38
0.0331	$Fe^{2+}(2M1)$	1.39	2.77	0.27	30.3	0.78
	$Fe^{2+}(M3)$	1.37	2.43	0.29	24.5	0.64
	$Fe^{2+}(2M2)$	1.40	1.88	0.40	15.7	0.41
	Fe_1^{3+}	0.66	0.72	0.36	29.5	0.77
	Fe_2^{3+}	—	—	—	—	—
0.0482	$Fe^{2+}(2M1)$	1.39	2.76	0.28	29.7	0.77
	$Fe^{2+}(M3)$	1.36	2.43	0.29	24.4	0.63
	$Fe^{2+}(2M2)$	1.37	1.86	0.39	15.6	0.41
	Fe_1^{3+}	0.64	0.71	0.39	30.3	0.79
	Fe_2^{3+}	—	—	—	—	—

N o t e. δ — isomeric shift, Δ — quadruple splitting, W — half-width of absorption line; S — relative square of summary spectrum component, N — iron concentration. *, **, *** — fractions 0.08 ÷ 0.063; 0.1 ÷ 0.08 and > 0.1 mm accordingly.

value lies between those values for Mg^{2+} and Fe^{2+}, that are typical for $M1$ and $M3$ sites, and those for Na^+ and Ca^{2+}, that are typical for $M4$ sites. That's why Mn^{2+} could occupy $M4$-site like in Mn-cummingtonite [23] and riebeckite [16] structures, as well as $M2$ site like in hornblendes [2] and some other amphiboles [16]. Perhaps Mn^{2+} could also fill $M1$ and $M3$ sites. For instance in taramites structure it was placed in site $M1$ [10, 16].

Let's note, that Fe^{2+} distribution between octahedral sites of investigated amphibole corresponds to the scheme $Fe^{2+}(M3) > Fe^{2+}(M1) > Fe^{2+}(M2)$. This distribution reflects high-temperature formation conditions of calcic amphiboles [9, 10, 16].

Iron octahedral cations distribution by NGR data. The NGR spectrum of magnesiohastingsite (Fig. 1, *a*) is divided into four doublets of quadruple splitting using the least squares method. Three of them — $Fe^{2+}(M1)$, $Fe^{2+}(M2)$ and $Fe^{2+}(M3)$ — are due to resonance absorption of gamma quanta by Fe^{2+} ions nuclei in corresponding octahedral positions $M1$, $M2$ and $M3$, and the fourth — by Fe_1^{3+} — Fe^{3+} in all these positions. The assumption of Fe^{3+} presence in several positions is based on widening of Fe_1^{3+} doublet lines. At the same time this widening could be caused by not uniform cationic environment of Fe^{3+} in $M2$ site. The last could concentrate the number of ions with various valences. The identification of the doublets obtained is based on X-ray data and results of previous NGR-spectroscopic research of calcic amphiboles [5–7, 17]. By means of optical spectroscopy it was shown that in calcic amphiboles structure $M4$ site could be occupied by Fe^{2+} [4]. This result has caused changes in approaches to NGR spectra decomposition and their interpretation by some authors [24, 26, 27]. By X-ray analysis we did not identity the occupation by Fe^{2+} cations of $M4$ sites in given amphibole. Calculation of different valency iron ions concentration (N) in structural positions is made basing on the equality of their resonant absorption factors in all nonequivalent octahedrons [1, 15]. These results together with other spectroscopic parameters are given in Tab. 1. Cations distribution between octahedral sites, obtained from the NGR spectrum analysis, is described by the following numerical values of formula units per one position: $M1 = 0.406\ Fe^{2+}$; $M2 = 0.185\ Fe^{2+} +$

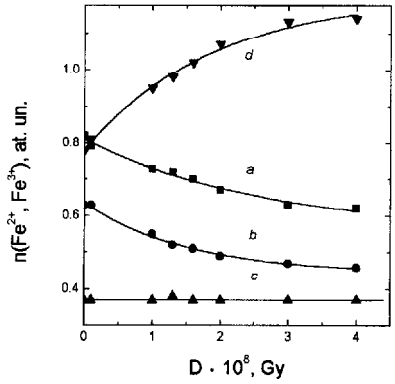

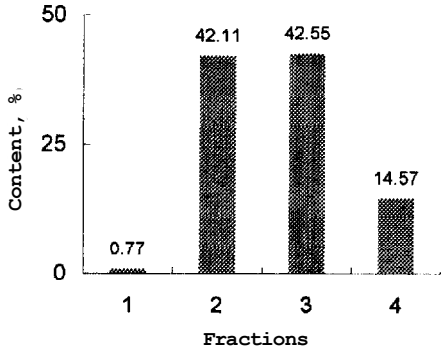

Fig. 2. Dependence of change of cations concentration of iron different valency on unequivalent structural positions magnesiohastingsite on a doze of an irradiation: *a* — $Fe^{2+}(2M1)$; *b* — $Fe^{2+}(M3)$; *c* — $Fe^{2+}(2M2)$; *d* — $Fe^{3+}(M1–3)$. Points — experimental values, continuous lines — theoretical curves designed on the equations 1, 2

Fig. 3. Distribution of grains magnesiohastingsite on fractions

$+0.39\ Fe^{3+}\ M3 = 0.63\ Fe^{2+}$. That is, the divergence of results on the octahedral sites occupancies by iron cations obtained by *X*-ray and NGR-spectroscopic data is ± 10 % and is within the limits of accuracy of both methods. Schemes of Fe^{2+} distribution between nonequivalent sites according to *X*-ray and NGR-spectroscopy data are identical. It is described by the typical for high-temperature genesis amphiboles set $Fe^{2+}(M3) > Fe^{2+}(M1) > Fe^{2+}(M2)$.

Influence of irradiation on iron cations valence state by NGR data. It is ascertained [6–8, 16, 19], that irradiation influence on structure and physicochemical properties of Fe- and OH-containing amphiboles is expressed in excitation of oxidation reactions of Fe^{2+} cations in octahedral *M*1 and *M*3 sites, coordinated by four anions O^{2-} and two OH^-. The radiation oxidation of iron is accompanied by geometrical distortions of coordination polyhedron. Iron oxidized by radiation is stable in environment conditions in time. On example of three Ca- and Na-amphiboles it was shown [5], that amphiboles susceptibility to iron oxidation under radiation influence depends on their structure and chemical composition. Iron oxidation in amphibole structure is accompanied by reduction of intensity of doublets $Fe^{2+}(M1)$, $Fe^{2+}(M3)$ and occurrence of a new doublet Fe_2^{3+}, characterized by high values of quadruple splitting and half-width of absorption lines (see Fig. 1, *b* – *d*; Tab. 1). The last doublet we attributed to radiation oxidated iron. Visible changes of spectra at small irradiation dozes ($0.01\cdot10^8$ and $0.1\cdot10^8$ Gy) are not marked. Therefore in this case Fe_2^{3+} doublet is not present in spectra. At decomposition into four doublets of the spectrum of the sample, irradiated by the doze $0.01\cdot10^8$ Gy, even 2.7 % reduction of doublet Fe_1^{3+} intensity relatively to initial sample spectrum is marked. It is the author's opinion that the last changes could be explained by the partial restoration of Fe^{3+} up to Fe^{2+} in quantity of 0.07 u. Similar effect was observed at the first stages of ferriferous elbaites experimental γ-irradiation [29]. Probably, such effects are also peculiar to amphiboles of other composition, irradiated by small dozes. Usually such changes lay within the limits of experimental measurement mistakes, and we do not fix attention on them. At irradiation doze increasing up to $4\cdot10^8$ Gy Fe^{3+} concentration increases from 0.78 in initial sample up to 1.14 at. un. in irradiated one, that is 14 % from the general iron contents. The change in the different valency iron cations contents in nonequivalent positions during irradiation is shown in a Fig. 2. Results of NGR-spectroscopic research of the sample, irradiated by the minimal doze $0.01\cdot10^8$ Gy, are not taken into account at the construction the given dependences . Analytically given dependences of change of Fe^{2+} concentration in positions *M*1 and *M*3, and Fe^{3+} concentration in all possible positions (curves *a*, *b*, and *d*) could be described by the exponential regression functions:

$$N = a + b\cdot\exp(-D/c), \qquad (1)$$

where the constant values, ensuring the best coincidence of experimental points and theoretical curves, correspondingly are: *a* — 0.562, 0.445 and 1.202; *b* — 0.249, 0.192 and –0.420; *c* —

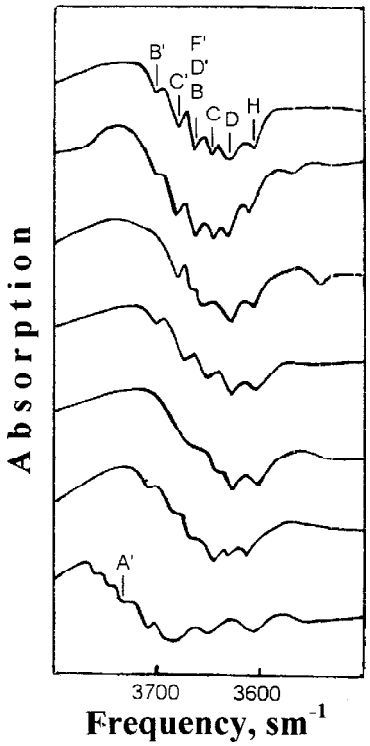

Fig. 4. IR-spectra of valent fluctuations OH of magnesiohastingsite. *Samples*: *1* — initial, *2 – 5* — irradiated by dozes $1\cdot10^8$, $2\cdot10^8$, $4\cdot10^8$ and $0.0331\cdot10^8$ Gy accordingly and received at room temperature; 1*a*, 4*a* — are received at temperature of liquid nitrogen; *1 – 4* — irradiation by a source ^{60}Co, *5* — in the wet channel of fuel assembly storehouse

$2.551\cdot10^8$ $1.489\cdot10^8$ and $1.879\cdot10^8$ Gy. The set of experimental points for Fe^{2+}(*M*2) (curve *c*) is described by linear function

$$N = a + b\cdot D, \qquad (2)$$

where $a = 0.372$ and $b = -2.474\cdot10^{-12}$ Gy^{-1}.

The comparison of functions (1) and (2) parameters values for given amphibole with those for taramite [7] testifies their dependence from the mineral composition.

To reveal the particles size influence on the intensity of the iron radiation oxidation processes, the sample, irradiated by the doze $4\cdot10^8$ Gy, is divided by the grains size into four fractions: 1 — < 0.063 mm; 2 — 0.08 ÷ 0.063; 3 — 0.1 ÷ 0.08; 4 — > 1 mm. The distribution of grains among the fractions is shown in Fig. 3. For fractions 2–4 the NGR spectrum are received. By results of several repeated measurements, when the mistake of definition is ≤ 1 %, the reduction of average values of total Fe^{3+} concentration from 45 up to 44.8 and 43.7 % for fractions 2–4 correspondingly is fixed. The reproducibility given during repeated experiments allows to conclude, that the amphibole crushing (limited by named particles dimensions) causes some intensification of iron radiation oxidation processes in its structure. This coincides with other authors conclusions about the influence of degree of samples dispersion on the radiating effects [25, 28].

The irradiation influence on anionic environment of iron cations by IR-spectroscopy data. IR-spectra are obtained on IR-spectrometer UR-20. For spectrum research in the 3500–3800 cm^{-1} spectral region samples were prepared as KBr pellets with 5 mg of the investigated substance. To exclude the spectrum distortions owing to the strong KBr hygroscopicity and to control them, spectra of thin films of the samples on the nonhygroscopic fluorite windows were also received. In the last case some vaseline oil was used to minimize the parasitic dispersion.

IR-spectrum of initial sample corresponds to spectra of hornblendes [13, 20]. In the 3500–3800 cm^{-1} region of hydroxyls stretching vibrations a wide weak absorption band has take place. The fine spectrum structure is represented, at least, by six overlapped narrow absorption bands. The most high-frequency absorption maximum is at the frequency 3700 cm^{-1}. According to R. G. Burns and R. G. J. Strens model [3], worked out for amphiboles with vacant *A* site, the most low-frequency absorption band would be at 3675 cm^{-1}. By this model it is attributed to stretching vibrations of hydroxyls, coordinated by three Mg atoms. I. L. Lapides and

Table 2. **Absorption bands frequencies of hydroxyls stretching vibrations in IR-spectra of magnesiohastingsite in 3500–3800 cm^{-1} spectral region**

Absorption band	Band maximum location, cm^{-1}	Cations in *M*1 and *M*3 sites	*A* site occupation
H	3610	$Fe^{2+}Fe^{2+}Fe^{3+}$	Vacant
D	3635	$Fe^{2+}Fe^{2+}Fe^{2+}$	"
C	3650	$Fe^{2+}Fe^{2+}Mg$	"
B		$Fe^{2+}MgMg$	"
D′	3668	$Fe^{2+}Fe^{2+}Fe^{2+}$	Occupied
F′		$Fe^{2+}Fe^{3+}Mg$	"
C′	3682	$Fe^{2+}Fe^{2+}Mg$	"
B′	3700	$Fe^{2+}MgMg$	"

T. A. Valjetov model [15] assumes, that the occupation of *A* site would give rise to the low-frequency shift of the appropriate hydroxyl stretching bands. The size of such shift depends on the sort of cations, that occupies *A* site, and on the degree of this site filling. According to crystallochemical formula of researched amphibole more then half of *A* sites are populated by K^+ and Na^+ ions that should lead to low-frequency hydroxyls stretchings displacement on 30–40 cm^{-1}. Hydroxyls stretching bands frequencies and their attribution according to model [15], that are displaced on 30–32 cm^{-1} relative to those offered by R. G. Burns and R. G. J. Strens, are given in Tab. 2.

The most intense in this frequency range is the band 3668 cm^{-1} (Fig. 4), which according to accepted model, corresponds to three overlapped bands with close frequencies that belong to the stretching vibrations of three differently coordinated hydroxyls: *B* —$\nu_{OH-Fe^{2+}Fe^{2+}Mg}$, in which the nearest adjacent *A* sites are vacant, *D*' — $\nu_{OH-3Fe^{2+}}$ and *F*'— $\nu_{OH-Fe^{2+}Fe^{3+}Mg}$ with the occupied *A* sites in their nearest environment. These bands attribution is in good agreement with chemical composition of studied amphibole.

The character of IR-absorption curve of γ-irradiated samples changes in the process of doze accumulation from $1 \cdot 10^8$ up to $4 \cdot 10^8$ Gy due to the gradual intensity reduction of three most low-frequency bands (Fig. 4), attributed mainly to vibrations of hydroxyls adjoined to the populated *A* sites (Tab. 2). And as far as the maximal irradiation doze is achieved, absorption bands 3700 and 3682 cm^{-1} could be fixed only in the spectrum, recorded at the liquid nitrogen temperature. The sample irradiation does not lead to appearance of new absorption bands. The weak band 3668 cm^{-1} in the spectra of samples accumulated maximal irradiation doze, probably, corresponds to the band *B* (Tab. 2).

Thus, IR-spectra analysis allows to conclude that γ-irradiation gives rise to the loss of only those hydroxyls that are adjoined to the populated *A* sites. But the maximal γ-irradiation doze $4 \cdot 10^8$ Gy, accumulated by the sample, appeared to be insufficient to remove all of them from the lattice. Partial dehydroxylation of magnesiohastingsite as a result of radiation influence is due to radiation oxidation of iron in *M*1 and *M*3 sites. Based on the data obtained, it is possible to assume, that the activation energy of iron oxidation process in these structural positions is higher for those Fe^{2+} ions that are located near the vacant *A* site. Processes of iron radiation oxidation and of OH-groups deprotonisation are known to pass simultaneously [19]. Reaction of exchange between hydrogen and iron is based on electron-donor-acceptor properties of iron ions and proton-donor-acceptor properties of hydroxyl ion:

$$Fe^{2+} + OH^- \leftrightarrow Fe^{3+} + O^- + H^-. \quad (3)$$

In IR-spectrum of the sample which has accumulated doze 0.0331 Gy at irradiation in the channel of fuel assembly storehouse, the gravity centre of absorption band is displaced to 3682 cm^{-1} comparing to initial sample spectrum, as well as the small reduction of intensity of 3668 cm^{-1} band is observed. These changes are opposite to those fixed in spectra of samples, irradiated by ^{60}CO and described above. It, apparently, could occur as a result of replacement of the *F*' band — $\nu_{OH-Fe^{2+}Fe^{3+}Mg}$ by the *C*' band — $\nu_{OH-2Fe^{2+}Mg}$, caused by Fe^{3+} reduction under the influence of weak γ-radiation with continuous spectrum of energies.

Thus, the results obtained make it possible to conclude that γ-irradiation first of all has an influence upon iron ions in *M*1 and *M*3 sites, adjacent to populated by Na^+ and K^+ cations *A* sites. The last can be explained by the capture of hydrogen deposition at radiation splitting of OH bonds and formation of $[(K, Na)\,H]_k$ complexes in *A* site after the scheme:

$$(K, Na)^+ + H^- \rightarrow [(K, Na)\,H]_k. \quad (4)$$

The opportunity of realization of such mechanism of radiation-chemical processes of iron cations oxidation and deprotonisation of their anionic environment was considered by us in [19]. Complexes $[(K, Na)\,H]_k$ at thermal dissociation could take part in reduction of iron oxidized by radiation and its anionic environment as OH-groups:

$$Fe^{3+} + O^- + [(K, Na)\,H]_k \rightarrow Fe^{2+} + OH^- + (K, Na)^+. \quad (5)$$

The thermal reduction of iron, oxidized by radiation, in Fe, OH-containing amphiboles is the typomorphic property of the irradiated minerals [6, 8, 18, 19]. The thermal stability fields of $[(K, Na)H]_k$ complexes and of iron, oxidized by radiation, are close to one another.

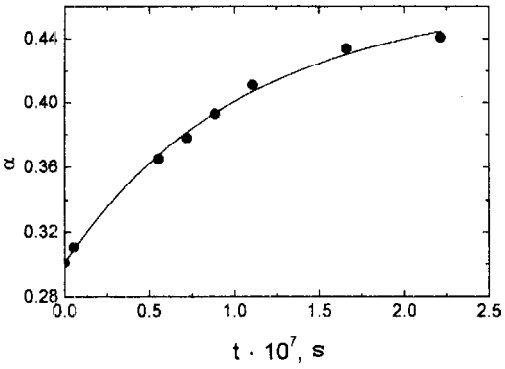

Fig. 5. Dependence of the relative contents Fe^{3+} in structure of magnesiohastingsite on time of its irradiation. Points — experimental values, continuous lines — theoretical curves designed on the equation (6)

Kinetics of Fe^{2+} radiation oxidation in magnesiohastingsite structure. Results of NGR-spectroscopic determination of the relative Fe^{3+} contents at the fixed doze of irradiation — $\alpha = (Fe^{3+}/Fe_{sum})$ are used to describe iron radiation oxidation kinetics. We had considered phenomenon of oxidized iron accumulation as a result of simultaneous iron oxidation and reduction processes that take place under irradiation influence. They have different intensity and are oppositely directed in time. α dependence from time of irradiation, according to our previous works [6, 7], is described by the equation:

$$\alpha = \alpha_\infty - [\alpha_\infty - \alpha_0] \exp[-(k_1 + k_2)t]. \quad (6)$$

Here $\alpha_\infty = [Fe^{3+}]_\infty/Fe_{sum}$ — relative quantity of Fe^{3+} at $t \to \infty$; $\alpha_0 = [Fe^{3+}]_0/Fe_{sum}$ — relative quantity of Fe^{3+} before the irradiation; k_1 and k_2 — constants of rate of oxidation and reduction correspondingly; t — time of irradiation, determined as $t = D/P$. The values obtained experimentally and calculated by the equation (6) are given in Tab. 3 and are shown in Fig. 5. The best coincidence of the experimental and theoretical data is fixed at values $\alpha_\infty = 0.463$ and $k_1 + k_2 = 9.567 \cdot 10^{-8}$ s^{-1}. The k_1 and k_2 values have been calculated by the formula:

$$\alpha_\infty = k_1/k_1 + k_2 \quad (7)$$

and have estimate up $k_1 = 4.43 \cdot 10^{-8}$ s^{-1}, and $k_2 = 5.137 \cdot 10^{-8}$ s^{-1}.

Among parameters described the radiation influence on specific structure, we have used the following: V — rate of relative change of Fe^{3+} amount in dependence from time of irradiation; G — amount of Fe^{3+} ions, formed under the influence on the sample of radiation energy unit; E — field energy, that is necessary to increase amount of Fe^{3+} ions on a unit. Formulas of their calculation have been considered in papers [6, 7], and their numerical values are given in Tab. 3. Dependence of each of these parameters from the irradiation time (doze) could be described by exponential function of regression. For the most informative parameter G, used for estimation of a mineral resistibility to radiating influences, such function looks like

$$G = a + b \cdot \exp(-D/c). \quad (8)$$

The best coincidence of the experimental points and the curve, described by the equation (8), is observed at the next constant values: $a = -1.519 \cdot 10^{10}$; $b = 1.162 \cdot 10^{15}$, $c = 1.888 \cdot 10^8$ Gy. Comparison of G values at the large irradiation dozes for investigated amphibole with those for

Table 3. **Dependence of kinetic parameters of iron radiation oxidation reactions from the radiation doze in magnesiohastingsite structure**

$D \cdot 10^8$, Gy	$t \cdot 10^7$, s	α_{exp}	α_{theor}	$V \cdot 10^{-9}$, s^{-1}	$G \cdot 10^{14}$, ion/J	ln$G$	$E \cdot 10^4$, eV/ion
0*	0	0.301	0.301	15.5	11.61	34.688	0.538
0.1	0.0554	0.311	0.309	14.7	11.01	34.635	0.568
1.0	0.554	0.365	0.368	9.122	6.833	34.158	0.915
1.3	0.7202	0.378	0.382	7.781	5.828	33.999	1.072
1.6	0.8864	0.393	0.394	6.637	4.972	33.840	1.257
2	1.108	0.411	0.407	5.369	4.022	33.628	1.554
3	1.662	0.434	0.430	3.16	2.367	33.098	2.640
4	2.216	0.441	0.444	1.86	1.393	32.568	4.486

N o t e. * — the values of parameters make sense at insignificantly to a small doze and time of irradiation, when D and $t \to 0$, and α_{exp} reflects a ratio of ions Fe of different valency, generically incorporated in structure of not irradiated minerals.

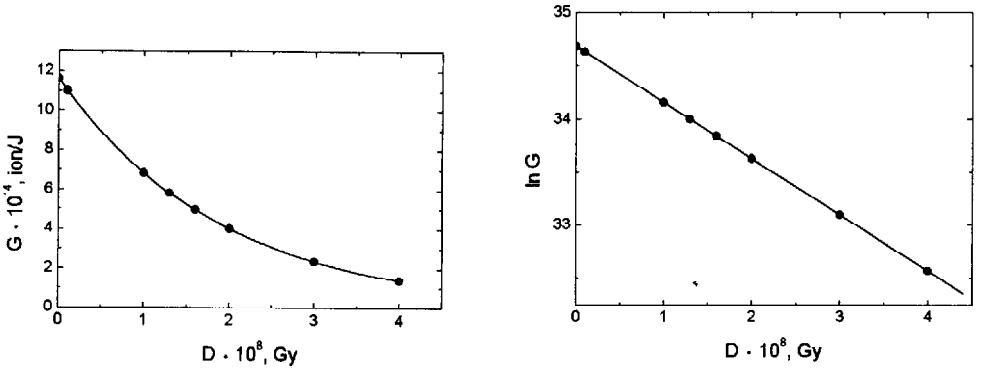

Fig. 6. Dependence of quantity of ions Fe^{3+}, unit, formed at influence, of energy of radiation on a sample, from a doze of an irradiation of magnesiohastingsite. Points — experimental values, continuous lines — theoretical curves designed on the equation (8)

Fig. 7. Dependence of ln (G) on a doze of an irradiation of magnesiohastingsite. Points — experimental values, continuous lines — theoretical curves designed on the equation (9)

magnesial and tschermakitic hornblendes, riebeckite and taramite, that are given in work [7], allows to establish the higher sensibility of magnesiohastingsite hornblende structure relatively to the first three minerals compared and reduced — relatively to the fourth one.

The logarithmic dependence of parameter G upon the irradiation doze as a straight line is more convenient for comparison with similar dependences of other minerals and for estimation of their relative resistibility to radiation influence. It looks like:

$$\ln G = a + bD, \qquad (9)$$

where the values of constants are $a = 34.688$; $b = -5.3 \cdot 10^{-9}$ Gy^{-1} under the R-factor values that are not less than 0.999. Comparison of slope ratio of straight lines $\ln G = f(D)$, describing the rate of Fe^{3+} accumulation in minerals structure, makes it possible to estimate by sight the crystal structures irradiation stability and to carry out the radiation loadings dosimetry of minerals under natural and man-caused influence of radiation fields.

Conclusions. 1. It is shown by means of X-ray analysis and NGR-spectroscopy, that octahedral sites in magnesiohastingsite structure are filled by Fe^{2+} cations in order $Fe^{2+}(M3) > Fe^{2+}(M1) > Fe^{2+}(M2)$, that reflects a high-temperature conditions of calcic amphiboles formation.

2. Formulas describing the changes in the different valence iron ions content in structural sites during the mineral irradiation are obtained.

3. Kinetics of Fe^{3+} accumulation in amphibole structure is described on the basis of the physical process model, proposed by the authors. Calculated kinetic parameters are the following: V — the rate of the relative change of Fe^{3+} number, that depends on the irradiation time; G — number of Fe^{3+} ions, formed under the influence on the sample of radiation energy unit; E — the field energy that is necessary to increase of the Fe^{3+} ions number per unit. Dependences of the mentioned above parameters from absorbed radiation doze could be used to estimate the relative radiation stability of minerals.

4. By means of IR-spectroscopy it is determined that Fe^{2+} radiation oxidation occurs mainly in $M1$ and $M3$ sites, adjacent to A sites populated by Na^+ and K^+ cations. This fact experimentally confirms our hypothesis of iron radiation oxidation and thermal reduction mechanisms, which were put forward earlier.

5. These results could be used for dosimetry of radiation loadings, and also for estimation of the possibility to use amphibole-bearing rocks as a burial place of RW.

1. *Bankroft G. M., Burns R. G.* Mössbauer and absorption spectral study of alkali amphiboles // Miner. Soc. Amer. Spec. Pap. — 1969. — Pap. 2. — P. 137–148.
2. *Batijevskiy B. A., Ivanitsky V. P., Litvin A. L. et al.* NGR spectra of hornblendes of ros-tikich series // Geol. Journ. — 1975. — **35**, No 6. — P. 54–60 (in Russian).
3. *Burns R. G., Strens R. G. J.* Infrared study of the hydroxyl bands in clinoamphiboles // Science. —

1966. — **153**, No 3738. — P. 890–892.
4. *Goldman D. S.* A reevaluation of the Mössbauer spectroscopy of calcic amphiboles // Amer. Miner. — 1979. — **64**, No 1/2. — P. 109–118.
5. *Goldman D. S., Wilson M. J.* A Mössbauer study of the weathering of hornblende // Clay Miner. — 1976. — **11**, No 1. — P. 153–163.
6. *Ivanitsky V. P., Voznyuk P. O., Lytovchenko A. S., Bondarenko G. N.* Investigation of radiation oxidation processes in iron in amphiboles and kinetics of their course (on NGR data) // Mineral. Journ. (Ukraine). — 2001. — **23**, No 1. — P. 42–54 (in Russian).
7. *Ivanitsky V. P., Voznyuk P. O., Legkova G. V., Lytovchenko A. S.* Kinetics of radiation-chemical oxidation in taramite and its radiation resistance // Ibid. — 2003. — **25**, No 2/3. — P. 27–34 (in Russian).
8. *Ivanitsky V. P., Kalinichenko A. M., Matyash I. V. et al.* Study of processes of thermal and radiation oxidation and dehydroxylation of hornblende by spectroscopy methods // Geochemistry. — 1977. — No 7. — P. 1073–1084 (in Russian).
9. *Ivanitsky V. P., Kalinichenko A. M., Matyash I. V. et al.* Iron ions distribution in hornblendes structure by NGR and PMR data // Mineral. Journ. (Ukraine). — 1980. — **2**, No 5. — P. 34–39 (in Russian).
10. *Ivanitsky V. P., Legkova G. V., Krivdik S. G.* Distribution octahedral cations in the structure of taramites from NGR-spectroscopy data // Ibid. — 2003. — **25**, No 1. — P. 62–67 (in Russian).
11. *Krivokonjeva G. K., Sidorenko G. A.* Influence of a radiation on some rockforming and ore minerals // Thes. Rept of All-Union Meeting "Radioactive elements in mountain breeds". — Novosibirsk, 1972. — Pt II. — P. 153–154.
12. *Krivokonjeva G. K., Skljadnjeva V. M., Bituljeva N. D.* Structural changes of ceramic materials under the action of neutron bombardment in conditions of high temperatures // Research of structure and phase contents of mineral objects by complex of physical methods for solution of technological tasks. — Moscow: VIMS, 1981. — P. 68–84 (in Russian).
13. *Kuznjetsova L. G., Lipatova A. L.* Infrared absorption spectra of main rockforming minerals (methodical instructions). — Leningrad: VSEGEI, 1973. — 109 p. (in Russian).
14. *Lasarenko E. K.* Importance of mineralogical research in solution of general geological problems // Mineral. Col.. Lvov Geol. Soc. — 1972. — No 2. — P. 123–140 (in Russian).
15. *Lapides I. L., Valjetov T. A.* Cations ordering in amphiboles. — Moscow: Nauka, 1986. — 124 p. (in Russian).
16. *Litvin A. L.* Crystallochemistry and structural typomorphism of amphiboles. — Kiev: Nauk. Dumka Press, 1977. — 236 p. (in Russian).
17. *Litvin A. L., Ivanitsky V. P., Ostapenko S. S. et al.* Influence of thermal treatment on structure and physico-chemical properties of gastingsite hornblende from rapakivi granites of Korosten pluton: Prepr. IGMOF. — Kiev, 1993. — 55 p. (in Russian).
18. *Litvin A. L., Ivanitsky V. P., Ostapenko S. S.* Radiation and heat effect on the structure of iron-containing Ca-amphibole // Mineral. Journ. (Ukraine). — 1994. — **16**, No 1. — P. 75–84 (in Russian).
19. *Matyash I. V., Kalinichenko A. M., Lytovchenko A. S. et al.* Radiospectroscopy of micas and amphiboles. — Kiev: Nauk. Dumka Press, 1980. — 188 p. (in Russian).
20. *Moenke H.* Mineralspectren. Bd 1, 2. — Berlin: Acad. Verlag, 1962. — 42 p., 355 charts.
21. *Nomenclature* of amphiboles // Can. Miner. — 1975. — **16**, No 5. — P. 501–520.
22. *Novikov G. V.* Method of analysis of louresolved spectra. — 1987. — 15 p. — Dep. in VINITI, No 4112-Б87.
23. *Papike J. J., Ross M., Clark J. R.* Crystal-chemical characterisation of clinoamphiboles based on five new structure refinements // Miner. Soc. Amer. Spec. Pap. — 1969. — No 2. — P. 117–136.
24. *Scogby H., Ferrow E.* Iron distribution and structural order in synthetic calcic amphiboles studied by Mössbauer spectroscopy and HRTEM // Amer. Miner. — 1989. — **74**, No 3-4. — P. 360–366.
25. *Syomka V. V., Lytovchenko A. S., Shekhynova S. B.* Study of radiation defects in γ-irradiated halite by EPR-method // Mineral. Journ. (Ukraine). — 2003. — **25**, No 2/3. — P. 35–40 (in Russian).
26. *Taran M. N., Andrut M., Polshin E. V., Matsyuk S. S.* Optical spectroscopy study of natural Fe, Ti-bearing calcic amphiboles // Phys. and Chem. Miner. — 1999. — **27**, No 1. — P. 59–69.
27. *Thomas W. M.* Fe^{57} Mössbauer spectra of natural and synthetic hastingsites, and implications for peak assignments in calcic amphiboles // Amer. Miner. — 1982. — **67**, No 5-6. — P. 558–567.
28. *Vovk I. F.* Subtraction of chemical elements from rock forming minerals and mountain rocks under the influence of a radioactive irradiation // Rept of Acad. of Sci. of Ukr.SSR. Ser. B. — 1972. — No 4. — P. 305–308 (in Russian).
29. *Voskresenskaya I. E., Korovushkin V. V., Moisejev B. M., Shipko M. P.* Mössbauer research of γ-irradiated ferriferrous elbaites // Crystallography. — 1979. — **24**, No 4. — P. 835–837 (in Russian).

Inst. of Geochemistry, Mineralogy and Ore Formation
of Nat. Acad. of Sci. of Ukraine, Kyiv
Inst. of Inform.-Diagnostic Systems of Nat. Aircraft Univ., Kyiv
Ukr. State Technol. Univ. of Food Technologies, Kyiv

Received 13.04.2004

РЕЗЮМЕ. Методами рентгеноструктурного аналізу, ЯГР- та ІЧ-спектроскопії вивчено розподіл октаедричних катіонів по нееквівалентних позиціях магнезіогастингситу. Зміна вмісту іонів заліза різної валентності по структурних позиціях і кінетика накопичення Fe^{3+} у процесі опромінення описані з

використанням математичних рівнянь. Розраховані кінетичні параметри, які дозволяють оцінювати сприйнятливість мінералів до радіаційного впливу. Встановлена залежність ефектів радіаційного впливу від розмірів частинок опромінюваного мінералу. Показано, що радіаційне окиснення заліза відбувається переважно у позиціях *M*1 и *M*3, що розташовані поблизу позицій *A*, заповнених іонами K^+ та Na^+. Це дозволило розвинути гіпотезу про механізми радіаційного окиснення заліза і дегідроксилації його оточення, а також їхнього термічного відновлення. Отримані результати важливі для дозиметрії радіаційних навантажень, а також для оцінки здатності амфіболвмісних порід для захоронення радіоактивних відходів.

РЕЗЮМЕ. Методами рентгеноструктурного анализа, ЯГР- и ИК-спектроскопии изучено распределение октаэдрических катионов по неэквивалентным позициям в структуре магнезиогастингсита. Изменение содержания ионов железа разной валентности в структурных позициях и кинетика накопления ионов Fe^{3+} в процессе облучения описаны с использованием математических уравнений. Рассчитаны кинетические параметры, позволяющие оценивать восприимчивость минералов к радиационным воздействиям. Установлена зависимость эффектов радиационного воздействия от размеров частиц облучаемого минерала. Показано, что радиационное окисление железа происходит преимущественно в позициях *M*1 и *M*3, которые расположены вблизи позиций *A*, заполненных ионами K^+ и Na^+. Это позволило развить гипотезу о механизмах радиационного окисления железа и дегидроксилации его окружения, а также их термического восстановления. Полученные результаты важны для дозиметрии радиационных нагрузок, а также для оценки пригодности амфиболсодержащих пород для захоронения радиоактивных отходов.